

## DART WARS

D. Di Bari (Tecn.), D. Di Gioacchino, C. Gatti, C. Ligi (Resp. Loc.), G. Maccarrone,  
G. Papalino(Tecn.), L. Piersanti, G. Pileggi (Tecn.), A. Rettaroli (Dott.),  
S. Tocci (AR)

### 1 Introduction

Noise at the quantum limit over a large bandwidth is a fundamental requirement for future applications operating at millikelvin temperatures, such as the neutrino mass measurement, the next-generation x-ray observatory, the CMB measurement, the dark matter and axion detection, and the rapid high-fidelity readout of superconducting qubits. The read out sensitivity of arrays of microcalorimeter detectors, resonant axion-detectors, and qubits, is currently limited by the noise temperature and bandwidth of the cryogenic amplifiers. The DARTWARS (Detector Array Readout with Traveling Wave Amplifiers) project has the goal of developing high-performing innovative traveling wave parametric amplifiers (TWPAs) with a high gain, a high saturation power, and a quantum-limited or nearly quantum limited noise. The practical development follows two different promising approaches, one based on the Josephson junctions and the other one based on the kinetic inductance of a high-resistivity superconductor <sup>1</sup>).

### 2 Characterization of first TWJPA samples at COLD-LNF

In the first semester of 2021 chips with TWJPA, JJ-based TWPA, produced at INRiM were tested at LNF, in collaboration with INRiM team, and at IBS-CAPP at about 10 mK in dilution refrigerators fully instrumented for RF measurements (figure 1). The Josephson metamaterial (shown in figure 2) is composed of 15 sections of coplanar waveguide embedding rf-SQUIDs connected by bended sections of CPW. The whole device contains 990 non-hysteretic rf-SQUIDs, characterised by values for the circuit parameters: ground capacitance  $C_g=13.0$  fF, geometrical inductance  $L_g=45$  pH, Josephson capacitance  $C_J=25.8$  fF and Josephson critical current  $I_c=1.5$   $\mu$ A. The values of  $L_g$  and  $C_J$  have been obtained by means of finite elements simulations, while  $I_c$  has been estimated taking into account the junction area ( $0.4\mu\text{m}$ , measured by means of Scanning Electron Microscopy) and the junction critical current density, estimated using an empirical curve, obtained after the switching current measurement of Josephson junctions fabricated with the same technique, which relates the junction critical current density with the oxidation time and oxygen pressure used for the creation of the oxide barriers <sup>2</sup>).

The characterization of the realized rf-SQUID-based JTWPA in terms of its three wave mixing (3WM) capabilities and gain evaluated via pump-on pump-off technique has been carried out. Fig. 3 shows a scheme of the experimental setup used for the cryogenic characterization. In order to quantify nonlinear mixing effects, a 2 tones measurement is performed by supplying in input a weak signal tone (supplied by port 1 of an Agilent E5071C 300 kHz-20 GHz VNA) and a driving pump tone (coming from a Rohde&Schwarz SMA100B 8kHz-20 GHz signal generator). Microwave signals enter to a dilution refrigerator and pass through several attenuation stages, getting to the metamaterial at 10 mK after passing a directional coupler (Mini-Circuits ZUDC10-02183-S+) and

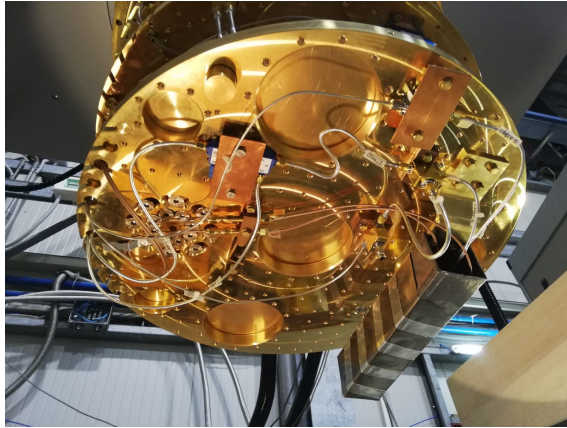


Figure 1: Setup of the 10 mK plate of the LNF cryostat for the characterization of the TWJPA.

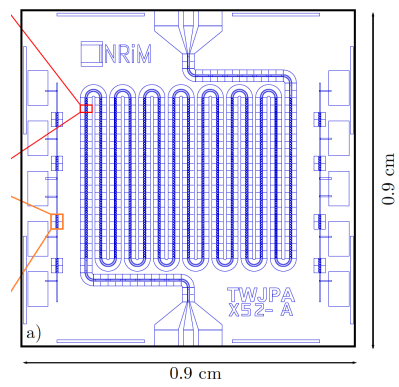
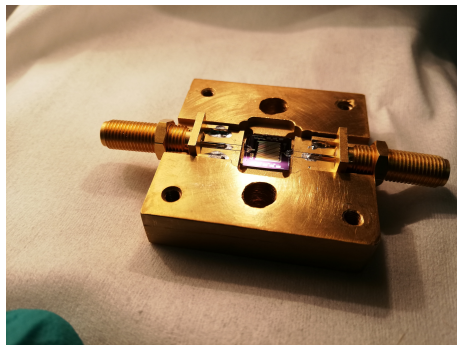


Figure 2: Left: LNF sample holder with the TWJPA chip bonded inside. Right: sketch of the TWJPA.

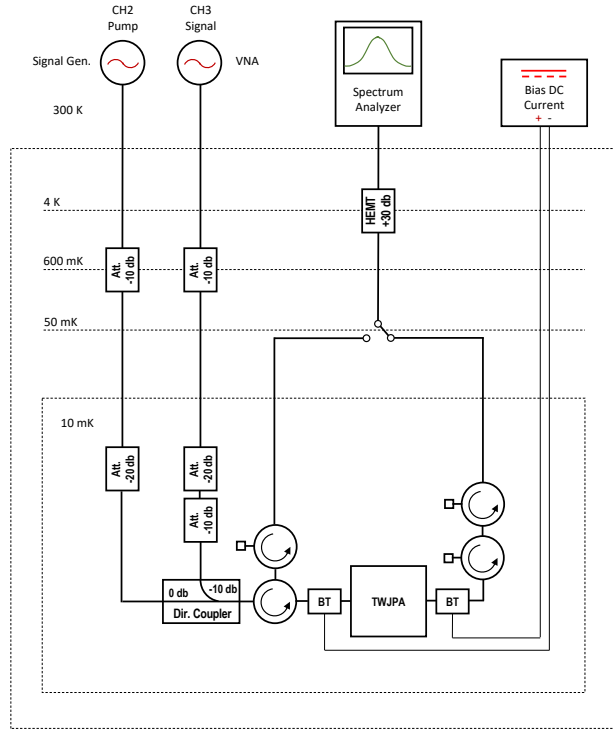


Figure 3: Schematic of the experimental setup used for the power and S parameters measurements.

a first isolation stage provided by a circulator (LNF-CIC412A). The microwave tones are then detected at room temperature after passing through a High Electron Mobility Transistor (HEMT, (LNF-LNC620C)) amplifier placed on the 4 K stage, which provides 30 dB of amplification. At room temperature a splitter, not shown, allows choosing, as a receiver, a spectrum analyzer (Signal Hound SM200B 100kHz-20 GHz) or port 2 of the VNA. This permits to perform power-spectra or scattering parameters measurements, respectively. A cryogenic electromechanical switch allows to adapt the setup for transmission or reflection measurements. In both configurations, the output microwave passes through an isolation stage realized by means of two circulators (LNF-CIC412A). A current generator (Keithley 6221) connected to the device via a couple of bias tees (Marki BT-0018) provides the DC current bias to the device.

In Fig. 4 we show the amplitude of the 3WM and 4WM idlers measured as a function of the DC bias current ranging between  $-50\mu\text{A}$  and  $+50\mu\text{A}$ . The pump tone is set to 6.8 GHz with power of  $-52$  dBm while the signal tone is set to 3.3 GHz with power of  $-64$  dBm, all referred to the amplifier input, and this sets the 3WM idler frequency to 3.5 GHz and the 4WM idler to 10.3 GHz. The possibility to send a DC current to the RF-SQUIDS in the TWJPA allows to tune their nonlinearity in order to generate 4WM and 3WM processes. When the DC bias current flows through the nonlinear transmission line, the inductance of each cell changes, in a periodic

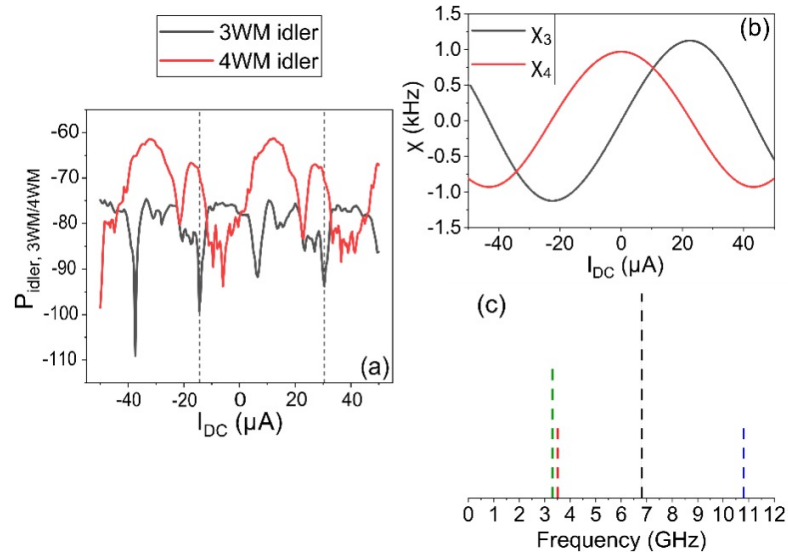


Figure 4: Plot (a) shows the power of the 3WM and 4WM idlers measured with a spectrum analyzer as a function of the DC bias current ranging between  $-50\mu\text{A}$  and  $+50\mu\text{A}$ . The pump tone is set to 6.8 GHz with power  $-52$  dBm while the signal tone is set to 3.3 GHz with power  $-64$  dBm, this sets the 3WM idler frequency to 3.5 GHz and the 4WM idler to 10.3 GHz. The two dashed vertical lines show the repetition of a period, whose length is  $46\mu\text{A}$ . Plot (b) represents the quadratic 3 and cubic 4 nonlinear coefficients that modulate the intensity of respectively the 3WM and 4WM idlers. The curves are calculated using the same circuit parameters of the metamaterial and results a period of  $46\mu\text{A}$  for the nonlinearity modulation. Figure (c) represents a scheme of the frequencies used and detected during the measurements of the data shown in Figure (a). The dashed lines represent the frequencies corresponding to the pump (black), signal (green), 3WM (red) and 4WM (blue).

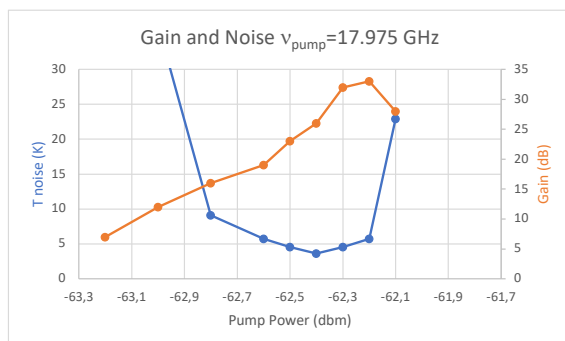


Figure 5: Gain (yellow) and noise (blue) measured as a function of the pump power for the TWJPA.

manner due to the SQUID behavior. The periodicity corresponds ideally, in our device, to  $46 \mu\text{A}$ , the distance between the two vertical dashed lines in Fig. 4. This modifies the nonlinearity of the transmission line, allowing 3WM and 4WM modes of operation, and clearly demonstrate the possibility to tune the TWJPA device with a simple DC current to activate the wanted mixing process. According to analytical models, the modulation of the signal levels reported in Fig. 4 should be strictly periodic, with the period indicated by the dashed lines. This is only partially true in the experiments, the deviation being attributed to scattering of the circuit parameters in the device fabrication. The detailed understanding of the deviation of the experimental data from the expected ones is under investigation. Fig. 5 reports the measured response of the TWJPA operating in the 3WM mode. The pump frequency is fixed at 17.975 GHz and its amplitude is swept from  $-63.3 \text{ dBm}$  to  $-61.8 \text{ dBm}$ . The signal gain is reported by the yellow curve and right axis, while the corresponding noise temperature, of the whole RF chain, by the blue curve and left axis. Signal gain and noise have been calibrated by measuring the coaxial lines attenuation and HEMT gain both at room temperature and during cryostat operation. The estimated error is 2 dB in gain and 1.5 K in noise temperature. The best resulting value is, in terms of noise temperature, 4K, with a gain of 25 dB. This is not satisfactory and is most probably due to a, later discovered, malfunctioning of the employed attenuators at low temperatures. Moreover, we have indication of a significative impedance mismatch between the input and output coaxial lines and the TWJPA amplifier. This introduces non ideal bandwidth and gain responses. However, the preliminary result reported here is encouraging as it gives clear clues for improvement of the amplifier performances <sup>3)</sup>.

### 3 Publications

- A. Rettaroli et al., “Microwave Quantum Radar using a Josephson Traveling Wave Parametric Amplifier,” arXiv:2111.03409.
- L. Fasolo et al., ”Bimodal Approach for Noise Figures of Merit Evaluation in Quantum-Limited Josephson Traveling Wave Parametric Amplifiers,” in IEEE Transactions on Applied Superconductivity, doi: 10.1109/TASC.2022.3148692, arXiv:2109.14924.
- A. Giachero et al., “Detector Array Readout with Traveling Wave Amplifiers,” arXiv:2111.01512.
- S. Pagano et al., ”Development of Quantum Limited Superconducting Amplifiers for Advanced Detection,” in IEEE Transactions on Applied Superconductivity, vol. 32, no. 4, pp. 1-5, June 2022, Art no. 1500405, doi: 10.1109/TASC.2022.3145782.

## **Acknowledgement**

Partially supported by EU through FET Open SUPERGALAX project, grant agreement N.863313

## **References**

1. A. Giachero et al., "Detector Array Readout with Traveling Wave Amplifiers," arXiv:2111.01512.
2. A. Rettaroli et al., "Microwave Quantum Radar using a Josephson Traveling Wave Parametric Amplifier," arXiv:2111.03409.
3. S. Pagano et al., "Development of Quantum Limited Superconducting Amplifiers for Advanced Detection," in IEEE Transactions on Applied Superconductivity, vol. 32, no. 4, pp. 1-5, June 2022, Art no. 1500405, doi: 10.1109/TASC.2022.3145782.